*Inorg. Chem.* **2004**, *43*, 4210–4215

# Exchange Interactions and Theoretical Analysis of $^{31}P$ NMR Spectra in $VO(HPO_4)\cdot 0.5H_2O$

**Sébastien Petit,[†] Serguei A. Borshch,[†] and Vincent Robert*[,†,‡]**

*Laboratoire de Chimie, UMR 5182, CNRS-Ecole Normale Supérieure de Lyon, 46, allée d'Italie, 69364 Lyon Cedex 07, France, and Université Claude Bernard Lyon I, 43, boulevard du 11 novembre 1918, 69622 Villeurbanne Cedex, France*

Received December 15, 2003

Based on combined *DFT/broken symmetry* approach, a theoretical analysis of the exchange interactions in the $VO(HPO_4)\cdot 0.5H_2O$ solid is performed. Depending on the crystallographic structures reported in the literature, two very different spin models are formulated. In addition, a complete fit of the temperature-dependent $^{31}P$ NMR chemical shift is performed to determine exchange and hyperfine constants. The magnetic models used in the fit are those obtained by our theoretical calculations. The comparison between the calculated and fitted exchange constants confirms the adequacy of an isolated dimer model and rules out the alternating antiferromagnetic chain model for $VO(HPO_4)\cdot 0.5H_2O$.

## 1. Introduction

The theoretical analysis of NMR spectra of magnetically coupled species presents rather complicated problems. The paramagnetic shift is mainly controlled by the spin density at the resonant nucleus and the hyperfine coupling strength.[1] In order to reproduce such spectra, one has to quantitatively characterize the three-dimensional scheme of magnetic interactions in the system. Therefore, a careful analysis of the magnetic data and NMR spectra should be extremely valuable when the question of the crystallographic structure is debated. In a recent series of papers,[2−5] we demonstrated that density functional theory (DFT) cluster calculations of magnetic coupling constants combined with numerical evaluations of hyperfine constants allow one to identify one particular phase of the vanadyl pyrophosphate $(VO)_2P_2O_7$ on the basis of its NMR spectra.

This compound is representative of oxovanadium phosphate V(+IV) solids which have attracted much attention in both the physical and chemical communities. The chemical importance of these materials stems from their participation as constituents or precursors of the active phase in highly efficient industrial catalysts used in the selective oxidation of the *n*-butane in maleic anhydride.[6] As the nature of the active site of these catalysts has not been clarified so far, a wide range of experimental[6−13] techniques including in particular magnetic susceptibility measurements and $^{31}P$ NMR has been called for to investigate the catalytic systems.

In solid state physics, the interest in oxovanadium phosphate V(+IV) compounds has grown from their intriguing magnetic properties which in many cases are likely to be analyzed on the basis of low-dimensional magnetic schemes. Each vanadium site in the formal oxidation state +IV has a $d^1$ electronic configuration and exhibits a local spin $^1/_2$. The richness of exchange pathways between these paramagnetic centers is responsible for a variety of networks of magnetic interactions. Thus, different magnetic models, ranging from

* Author to whom correspondence should be addressed. E-mail: vrobert@ens-lyon.fr. Fax: (33) 4 72 44 53 99.
† CNRS-Ecole Normale Supérieure de Lyon.
‡ Université Claude Bernard Lyon I.

(1) Bertini, I.; Luchinat, C. *Coord. Chem. Rev.* **1996**, *150*, 1.
(2) Lawson Daku, L. M.; Borshch, S. A.; Robert, V.; Bigot, B. *Chem. Phys. Lett.* **2000**, *330*, 423.
(3) Petit, S.; Borshch, S. A.; Robert, V. *J. Am. Chem. Soc.* **2002**, *124*, 1744.
(4) Petit, S.; Borshch, S. A.; Robert, V. *J. Solid State Chem.* **2003**, *170*, 237.
(5) Petit, S.; Borshch, S. A.; Robert, V. *J. Am. Chem. Soc.* **2003**, *125*, 3959.
(6) Centi, G. *Catal. Today* (special issue) **1993**, *16*, 1−147.
(7) Bordes, E. *Catal. Today* **1987**, *1*, 499.
(8) Abdelouahab, F. B.; Olier, R.; Guilhaume, N.; Lefebvre, F.; Volta, J. C. *J. Catal.* **1992**, *134*, 151.
(9) Li, J.; Lashier, M. E.; Schrader, G. L.; Gerstein, B. B. *Appl. Catal.* **1991**, *73*, 83.
(10) Abon, M.; Bere, K. E.; Tuel, P.; Delichère, A. *J. Catal.* **1995**, *156*, 28.
(11) Joly, J. P.; Méhier, C.; Béré, K. E.; Abon, M. *Appl. Catal. A* **1998**, *169*, 55.
(12) Cornaglia, L.; Irusta, S.; Lombardo, E. A.; Durupty, M. C.; Volta, J. C. *Catal. Today* **2003**, *78*, 291.
(13) Johnson, J. W.; Johnston, D. C.; Jacobson, A. J.; Brody, J. F. *J. Am. Chem. Soc.* **1984**, *106*, 8123.



10.1021/ic035437x CCC: $27.50 
Published on Web 06/05/2004

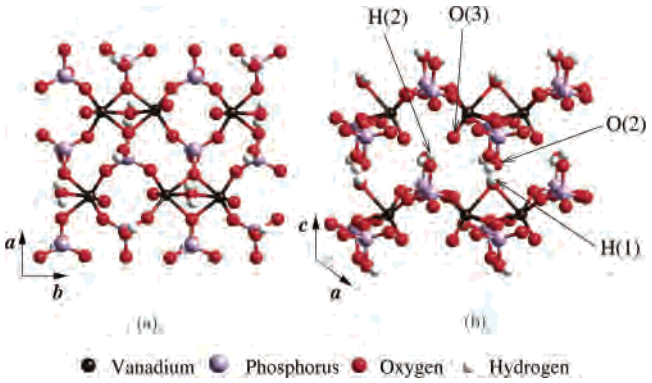


**Figure 1.** Crystallographic structure of VO(HPO4)·0.5$H_2O$ solid in (a) (*a*,*b*) plane and (b) (*a*,*c*) plane (ref 20).

isolated dimer to alternating dimer chain and 3-D systems, have been proposed in the literature for different oxovanadium phosphates.[3,4,13−19]

In the present paper, our interest is focused on one particular oxovanadium phosphate, $VO(HPO_4)\cdot 0.5H_2O$, namely, vanadyl hydrogenophosphate hemihydrate. All oxovanadium phosphate solids may be viewed as arrangements of distorted $VO_6$ octahedra and $PO_4$ tetrahedra linked together in various ways giving rise to numerous crystallographic structures. The hemihydrate $VO(HPO_4)\cdot 0.5H_2O$ solid consists of chains of $VO_6$ octahedra along the *b* axis organized in a layered structure (Figure 1). The chains can be viewed as the alternation of vanadium dimers with double O−P−O bridge and di-$\mu$-oxo bridge. In the *c* direction, the stacking comes from two types of hydrogen bonds. One hydrogen atom (H(1) in Figure 1) of a water molecule is involved in such bonding along with the oxygen atom (O(2)) of a $PO_4$ group. The second link results from the binding of the structural hydrogen H(2) to the vanadyl oxygen atoms O(3) (Figure 1). $VO(HPO_4)\cdot 0.5H_2O$ solid as well as its deuterium analogue were subject to several crystallographic studies.[13,20−24] Different preparation procedures were used in these studies, and the data were obtained either on single crystal[20,21] or powder samples.[13,22−24] In the meantime, different structures were determined for several temperatures ranging from 10 K up to 583 K.[13,20−24] Structural works agree on an orthorhombic $P_{mmn}$ symmetry group consisting of one vanadium atom in the unit cell and with almost temperature-independent lattice parameters. One singularity appears at 143 K where Torardi et al.[20] suggested a $P2_1/c$ space group with a doubled elementary cell along the *c* direction containing two different nonequivalent vanadium atoms. The room-temperature structure exhibits a positional disorder of O(2) and O(3) oxygen atoms[20,21] which disappears at lower temperatures.[20] One should mention that such doubling of the unit cell has not been reported for the deuterated $VO(DPO_4)\cdot 0.5D_2O$ analogue.[22,23] Even though different experimental conditions were used, only small structural variations of distances or angles were reported.

**Table 1.** Exchange Constants Determined by Different Methods for the $VO(HPO_4)\cdot 0.5H_2O$ Compound[a]

| *J* (K) | method | ref |
|---|---|---|
| 91 ($D_O$) | $\chi(T)$ | 13 |
| 88 ($D_O$) | $\chi(T)$ | 25 |
| 86 ($D_O$) | $\chi(T)$ | 15 |
| 91 ($D_{OPO}$) | INS | 22 |
| 122 (intrachain $D_{OPO}$), 77 ($D_O$), −8 (interchain $D_{OPO}$), −3 (M) | DFT | 4 |

[a] In parentheses, we give the proposed assignment of exchange constants. Positive *J* values correspond to antiferromagnetic exchange interaction.

On the other hand, the magnetic properties of $VO(HPO_4)0.5H_2O$ were studied by different experimental techniques[13,15,22,25−27] and analyzed on the basis of quantum chemical calculations.[4,29,30] The magnetic interaction scheme and the assignment of experimental exchange constants are largely debated in the literature. The magnetic susceptibility[13,15,25] and INS[22] data were fitted by an isolated antiferromagnetic dimer model with exchange parameters listed in Table 1.

Since the INS data[22] also allow the determination of the distance between the magnetic centers forming the dimer, it was suggested that the exchange interaction spreads through the long O−P−O bridge and not through the short $\mu$-oxo bridge. However, extended Hückel calculations,[29,30] which estimate the relative effectiveness of the exchange pathways through the HOMO−LUMO gap values, led to an opposite conclusion. Our most recent DFT calculations[4] based on the Guliants et al. structural data also showed that the most efficient exchange interaction occurs through the O−P−O bridge (Table 1). However, the antiferromagnetic exchange coupling through the oxygen bridges has a comparable value, thus leading to another 1-D magnetic model, namely, the so-called alternating dimer chain model. Our *DFT* calculations[4] also suggested the presence of small interchain ferromagnetic interactions.

Several sets of NMR data, obtained for different temperature ranges, are available in the literature.[15,26−28] The data

(14) Johnston, D. C.; Johnson, J. W.; Goshorn, D. P.; Jacobson, A. J. *Phys. Rev. B* **1987**, *35*, 219.
(15) Beltrán-Porter, D.; Beltrán-Porter, A.; Amorós, P.; Ibañez, R.; Martinez, E.; Le Bail, A.; Ferrey, G.; Villeuneuve, G. *Eur. J. Solid State Inorg. Chem.* **1991**, *28*, 131.
(16) Garrett, A. W.; Nagler, S. E.; Tennant, D. A.; Sales, B. C.; Barnes, T. *Phys. Rev. Lett.* **1997**, *79*, 745.
(17) Kikuchi, J.; Motoya, K.; Yamauchi, T.; Ueda, Y. *Phys. Rev. B* **1999**, *60*, 6731.
(18) Barnes, T.; Riera, J.; Tennant, D. A. *Phys. Rev. B* **1999**, *59*, 11384.
(19) Johnston, D. C.; Saito, T; Azuma, M.; Takano, M.; Yamauchi, T.; Ueda, Y. *Phys. Rev. B* **2001**, *64*, 134403.
(20) Torardi, C. C.; Calabrese, J. C. *Inorg. Chem.* **1984**, *23*, 1308.
(21) Leonowicz M. E.; Johnson, J. W.; Brody, J. F.; Shannon, H. F.; Newsam, J. M. *J. Solid State Chem.* **1985**, *56*, 370.
(22) Tennant, D. A.; Nagler, S. E.; Garrett, A. W.; Barnes, T.; Torardi, C. C. *Phys. Rev. Lett.* **1997**, *78*, 4998.
(23) Garrett, A. W. Ph.D. Thesis, University of Florida, 1998.
(24) Guliants, V. V.; Holmes, S. A.; Benziger, J. B.; Heaney, P.; Yates, D.; Wachs, I. E. *J. Mol. Catal. A: Chem.* **2001**, *172*, 265.
(25) Johnston, D. C.; Johnson, J. W. *J. Chem. Soc., Chem. Commun.* **1985**, *23*, 1720.
(26) Furukawa, Y.; Iwai, A.; Kumagai, A.; Yakubovsky, K. *J. Phys. Soc. Jpn.* **1996**, *65*, 2393.
(27) Kikuchi, J.; Aoki, T.; Motoya, K.; Yamauchi, T.; Ueda, Y. *Physica B* **2000**, *284−288*, 1481.
(28) Sananes, M. T.; Tuel, A. *J. Chem. Soc., Chem. Commun.* **1995**, *13*, 1323.
(29) Roca, M.; Amorós, P.; Cano, J.; Marcos, M. D.; Alamo, J.; Beltrán-Porter, A.; Beltrán-Porter, D. *Inorg. Chem.* **1998**, *37*, 3167.
(30) Koo, H. J.; Whangbo, M. H.; VerNooy, P. D.; Torardi, C. C.; Marshall, W. J. *Inorg. Chem.* **2002**, *41*, 4664.

were analyzed assuming the proportionality between the paramagnetic shift value and the magnetic susceptibility and first favored the isolated dimer model.[15,26] However, recent experiments on the magnetic-field dependence of the $^{31}$P nuclear spin−lattice relaxation rate favored the alternating dimer chain model.[27] In our recent work,[5] a fit of the NMR data available for the high-temperature region (150−300 K)[28] was realized using calculated DFT exchange parameters. The hyperfine constants and the temperature-independent part of the chemical shift were taken as fitting parameters. We were able to correctly reproduce the main features of the chemical shift vs temperature curve in the low-temperature region[26] (i.e., the maximum position and its value, general trends). However, the value of the temperature-independent part (≈−500 ppm) seems too high for the phosphorus nucleus.

In this paper, we intend to investigate the magnetic properties of the vanadyl hydrogenophosphate hemihydrate $VO(HPO_4)\cdot 0.5H_2O$ using different experimental structural data reported in the literature. Our goal is to clarify the contradictory conclusions regarding the magnetic models for this particular representative of the oxovanadium phosphate family. First, based on mixed DFT/broken symmetry (BS) calculations, a mapping of the exchange constants is performed for the crystallographic structures given by both Torardi et al.[20] and Tennant et al.[22,23] These calculations complete our previous studies[4] performed using the Guliants et al.[24] structural data. In our approach, we did not assume any particular dominating exchange pathway but we rather looked for all possible magnetic couplings. These calculated values define a magnetic model appropriate to each structure.

Then, the topologies of the formulated magnetic models are used to fit the temperature-dependent $^{31}$P NMR spectra. In this procedure, we consider the exchange constants as fitting parameters together with the hyperfine coupling constants and the temperature-independent part. The extracted exchange parameters are directly compared to the ab initio evaluations, thus validating the combined DFT/BS approach.

Finally, we will show that the combination of ab initio calculations and NMR spectra fitting can be extremely valuable in assigning an appropriate magnetic model for the $VO(HPO_4)\cdot 0.5H_2O$ solid.

## 2. Methodology and Computational Details

**Exchange Constant Calculations.** The analysis of magnetic properties in polynuclear systems is usually performed within the Heisenberg−Dirac−Van Vleck spin Hamiltonian (HDVV),

$$H = \sum_{\langle i,j \rangle} J_{ij}\mathbf{S}_i\cdot\mathbf{S}_j \qquad (1)$$

According to this equation, positive exchange constant $J_{ij}$ means antiferromagnetic coupling between the two sites. For dimeric clusters which can be extracted from the whole solid, this Hamiltonian simply reads

$$H = J\mathbf{S}_1\cdot\mathbf{S}_2 \qquad (2)$$

with $J = E_T - E_S$, where $E_T$ and $E_S$ are the two energy levels (triplet and singlet) of a pair of $d^1$ ions. An alternative to the demanding multideterminantal evaluation of $J$ constants[31,32] is given by the broken symmetry (BS) approach proposed by Noodelman et al.[33] The energy of a fictitious BS state representing a mixture of the pure singlet and triplet states with $M_S = 0$ can be directly calculated within the unrestricted DFT framework. It is known that the exchange constant for a two-magnetic electron system reads

$$J = \frac{2(E_{BS} - E_T)}{1 + S_{\alpha\beta}^{\ 2}} \qquad (3)$$

where $E_{BS}$ is the broken symmetry state energy and $S_{\alpha\beta}$ is the overlap integral between the spin−orbitals of α and $\beta$ spin projections of the BS solution.

All our exchange constant calculations were performed using the Gaussian 98 package,[34] with rather extended basis sets. Double-ζ Gaussian type orbitals (GTO) basis sets, namely, 6-31G, were used for H, O, and P atoms, including one polarization function for P atoms. As far as the V atoms are concerned, the effects of the core electrons up to 2p were accounted for with the Los Alamos pseudopotential. Double-ζ basis sets optimized for this particular effective core potential (ECP) were applied for the valence electrons. As in our earlier studies of the VPO phases,[3,4] we used the standard generalized gradient-corrected hybrid functional B3LYP, involving the exchange Becke three parameter functional and the Lee−Yang−Parr correlation one. The self-consistent field (SCF) procedure for the BS state is performed by starting from the converged triplet state and by then allowing the mixing of highest α and $\beta$ spin−orbitals. For both high-spin and BS states, we checked that the spin densities were mainly concentrated on the vanadium orbitals with a small fraction on the vanadyl oxygen orbitals. The overlap integrals $S_{\alpha\beta}$ were computed by a local software developed for specific Gaussian basis sets.

Since we do not deal with molecular systems but with extended solids, our approach consists of the extraction of dimer clusters from the crystallographic structures of $VO(HPO_4)\cdot 0.5H_2O$. In the present paper, we used the different crystallographic data reported in ref 20 at 143 K and refs 22 and 23 at 10 and 300 K for the deuterated compound. In the following, these structures will be referred to as TO and TE structures, respectively.

Using these data, all the positions of hydrogen/deuterium atoms are clearly determined. We did not use the 300 K structure obtained by Torardi et al.[20] since the observed disorder cannot be described within quantum chemical model. Besides, no a priori dominating exchange pathway was assumed and we explored all the possible pairs of adjacent vanadium atoms. Three types of dimers can be identified. In order to describe the exchange interaction along the *b* direction (Figure 1), we considered the two different dimers, $D_O$ (Figure 2) and $D^1_{OPO}$ (Figure 2) alternating along this direction.


(31) Calzado, C. J.; Cabrero, J.; Malrieu, J. P.; Caballol, R. *J. Chem. Phys.* **2002**, *116*, 3985.
(32) Calzado, C. J.; Cabrero, J.; Malrieu, J. P.; Caballol, R. *J. Chem. Phys.* **2002**, *116*, 2728.
(33) Noodleman, L.; Case, D. A. *Adv. Inorg. Chem.* **1992**, *38*, 423.
(34) Frisch, M. J.; Trucks, G. W.; Schlegel, H. B.; Scuseria, G. E.; Robb, M. A.; Cheeseman, J. R.; Zakrzewski, V. G.; Montgomery, J. A.; Stratmann, R. E.; Buran, J. C.; Dapprich, S.; Millam, J. M.; Daniels, A. D.; Kudin, K. N.; Strain, M. C.; Farkas, O.; Tomasi, J.; Barone, V.; Cossi, M.; Cammi, R.; Mennuci, B.; Pomelli, C.; Adamo, C.; Clifford, S.; Ochterski, J.; Peterson, G. A.; Ayala, P. Y.; Cui, Q.; Mokuma, K.; Malick, D. K.; Rabuk, A. D.; Raghavachari, K.; Foresman, J. B.; Cioslowski, J.; Ortiz, J. V.; Stefanov, B. B.; Liu, G.; Liashenko, A.; Piskorz, P.; Komaromi, I.; Gomperts, R.; Martin, R. L.; Fox, D. J.; Keith, T.; Al-Laham, M. A.; Peng, C. Y.; Nanayakkara, A.; Gonzalez, C.; Challacombe, M.; Gill, P. M. W.; Johnson, B. G.; Chen, W.; Wong, M. W.; Andres, J. L.; Head-Gordon, M.; Replogle, E. S.; Pople, J. A.; *Gaussian 98*, revision A.7; Gaussian, Inc.: Pittsburgh, PA, 1998.

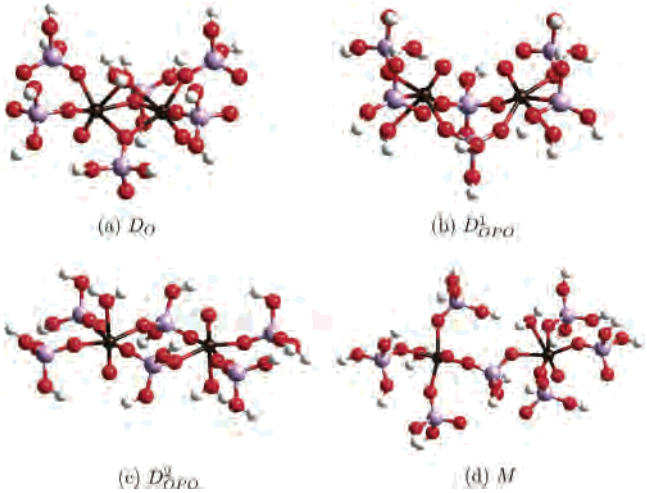


**Figure 2.** Dimers extracted from the crystallographic structures of $VO(HPO_4)\cdot 0.5H_2O$.

**Table 2.** V−V Distances (Å) and Bond Angles (deg) for the $D_O$ Dimers

| $D_O$ | $d$(V−V) | V−O−V |
|---|---|---|
| TO[20] | 3.09 | 97.1, 97.2 |
| TE,[22,23] 10 K | 3.09 | 97.6 |
| TE,[22,23] 300 K | 3.09 | 97.5 |
| GU[24] | 3.07 | 94.6 |

These dimers are referred to as intrachain dimers. The resulting chains are coupled together in ($a$,$b$) planes through $D^2_{OPO}$ (Figure 2) and M (Figure 2) interchain dimers. In order to illustrate the small geometry variations between different structural determinations, the most relevant distances and angles characterizing the bridges in the intrachain dimers are reported in Tables 2 and 3. For comparison, we give similar parameters taken from the crystallographic data published by Guliants et al.[24] (GU) used in our previous calculations.[4]

Finally, the environments of the magnetic vanadium atoms were explicitly included up to the third coordination spheres in each model dimer. The experimental structures were used without any optimization of the atomic positions. In order to ensure the electric neutrality of our model clusters, hydrogen atoms were attached to some oxygen atoms along the preexisting bonds with a standard O−H distance 0.95 Å.

**Paramagnetic Chemical Shift.** The interpretation of NMR data in compounds with a large number of interacting paramagnetic centers needs a preliminary detailed description of the electronic spin state manifold. The spin state energies $E_n$ characterized by the total spin $S_n$ and their eigenfunctions $|S_n\rangle$ can be obtained by the diagonalization of the relevant HDVV Hamiltonian (eq 1). The contribution of the paramagnetic center $M_i$ into the total temperature-dependent paramagnetic shift reads[1]

$$\delta_{M_i,\mathrm{para}}(T) = \frac{g\mu_B}{g_N\mu_N}\frac{A_{M_i}}{3k_BT}\times \frac{\sum_S\sum_n K_{M_i}(n)S(S+1)(2S+1)\exp\left(\frac{-E_n}{k_BT}\right)}{\sum_S\sum_n (2S+1)\exp\left(\frac{-E_n}{k_BT}\right)} = \frac{g\mu_B}{g_N\mu_N}\frac{A_{M_i}}{3k_BT}F_{M_i}(T) \quad (4)$$

where $A_{M_i}$ is the constant of hyperfine interaction of a resonant nucleus with the $M_i$ center. It is usually assumed that this constant does not depend on the interaction between the magnetic centers. The projection coefficients are given by

$$K_{M_i}(n) = \frac{\langle S_n|\mathbf{s}_i\cdot\mathbf{S}|S_n\rangle}{\langle S_n|\mathbf{S}\cdot\mathbf{S}|S_n\rangle} \quad (5)$$

where $\mathbf{s}_i$ is the electronic spin operator on center $M_i$ and $\mathbf{S}$ is the total spin operator. In eq 4, the summation runs over all the energy levels within each $S$ manifold. Since the hyperfine interactions decay rapidly with the distance, the total paramagnetic shift is obtained by summation over the nearest $M_i$ neighbors. In order to evaluate the energies and the spin eigenfunctions, one must define a magnetic model characterized by a minimal number of exchange constants.

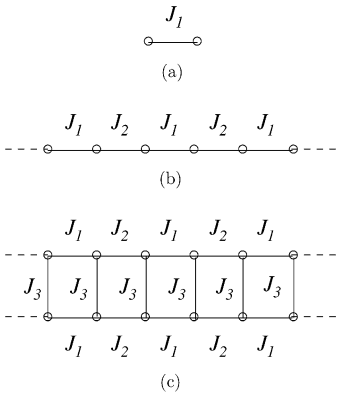


**Figure 3.** Magnetic clusters used in the $F_{M_i}(T)$ calculations based on (a) an isolated dimer model, (b) an alternating dimer chain model, and (c) coupled dimer chain model.

**Table 3.** V−V Distances (Å) and Selected Bond Angles (deg) for the Intrachain $D^1_{OPO}$ Dimers

| $D^1_{OPO}$ | $d$(V−V) | V−O−P | O−P−O |
|---|---|---|---|
| TO[20] | 4.32 | 141.7, 142.8, 154.5, 155 | 115.5, 115.6 |
| TE,[22,23] 10 K | 4.32 | 147.5 | 120.7 |
| TE,[22,23] 300 K | 4.33 | 149.6 | 114 |
| GU[24] | 4.35 | 150.5 | 113.7 |

In this work, three models of different degrees of complexity will be considered (Figure 3). These models were analyzed in our previous calculations[4] of exchange parameters for the structure reported in ref 24. For the isolated dimer model (Figure 3a), the determination of the energies values and spin states is straightforward. On the other hand, the alternating dimer chain (Figure 3b) and the system of coupled dimer chains (Figure 3c) require approximate treatment. The coupled dimer chain model is considered in order to evaluate the effects of interchain interactions.

Our approach consists in the exact diagonalization of the HDVV Hamiltonian built on finite size clusters with periodic boundary conditions. As shown in our previous paper,[5] a six magnetic center cluster description in the chain gives a satisfactory approximation of the temperature-dependent $F_{M_i}(T)$ functions (eq 4). In the $VO(HPO_4)\cdot 0.5H_2O$ compound, the phosphorus atom leading to a single signal experimentally observed in the NMR spectrum is surrounded by four vanadium atoms. Assuming that the $F_{M_i}(T)$ functions are identical for all the vanadium atoms ($F^{\mathrm{hemi}}(T)$), the final expression for the chemical shift can be written as

$$\delta(T) = \delta_{\mathrm{dia}} + \delta_{\mathrm{para}}(T) = \delta_{\mathrm{dia}} + \frac{\mathcal{C}}{T}A\cdot F^{\mathrm{hemi}}(T) \quad (6)$$

**Table 4.** Calculated Exchange Constants in $VO(HPO_4)\cdot 0.5H_2O$ Solid[a]

| | $J$ (K) | | | |
|---|---|---|---|---|
| crystal structure | $D_O$ | $D^1_{OPO}$ | $D^2_{OPO}$ | M |
| TO[20] | −11 | 131 | [−8.5; −9] | [−2; 3.5] |
| TE,[22,23] 10 K | −3 | 177 | −10 | −4 |
| TE,[22,23] 300 K | −1 | 145 | −10 | −4 |
| GU* [24] | 77 | 122 | −8 | −3 |

[a] The asterisk indicates the values calculated previously in ref 4.

where $\delta_{dia}$ is the temperature-independent part and

$$\mathscr{C} = \frac{g\mu_B}{3k_B g_N \mu_N}$$

In our previous work,[5] we had used the experimental NMR spectra between 150 and 300 K[28] to extract a sum of hyperfine constants and the temperature-independent contribution to the chemical shift. The exchange constants were calculated using another crystallographic structure.[24] However, the recent NMR data recorded between 4 and 280 K[27] contain enough experimental points to perform a complete fit of the hyperfine as well as the exchange constants. The adjustment was performed by minimizing the $\mathscr{R}$ function with a simplex algorithm:

$$\mathscr{R} = \frac{1}{N-n} \frac{\sum_j [\delta_{exp}(T_j) - (\delta_{dia} + \delta_{para}(T_j))]^2}{\sum_j [\delta_{exp}(T_j)]^2} \qquad (7)$$

where $N$ is the number of experimental points and $n$ the number of parameters we used.

### 3. Results and Discussion

**Ab Initio Exchange Constants.** From our calculations (Table 4), the most important exchange interaction in all studied structures of the $VO(HPO_4)\cdot 0.5H_2O$ compound is provided by the intrachain $D^1_{OPO}$ dimer (≈130−180 K). This result contradicts the conclusions drawn from previous extended Hückel calculations[29,30] which predicted the most important antiferromagnetic exchange for the $D_O$ dimer. In ref 30, the exchange constants were estimated using the magnetic orbital energies difference. In order to understand the origin of this discrepancy, we have calculated this energy difference $\Delta\epsilon$ between the highest occupied orbitals of the triplet state in the intrachain dimers of all hemihydrate structures. The $\Delta\epsilon$ values vary in the range 0.06−0.20 meV in $D_{OPO}$ dimers, whereas they are 0.01−0.02 meV in $D_O$ dimers. The opposite trend is observed using extended Hückel calculations.[30] Therefore, disagreement between our DFT approach and the extended Hückel based method can be expected. However, our calculations are in agreement with the experimental INS studies.[22]

The intrachain coupling through $\mu$-oxo bridges and the interchain interactions described by the $D^2_{OPO}$ and the $M$ dimers have smaller values and are of ferromagnetic nature ($J < 0$). As it follows from our calculations, the spin density is concentrated on the vanadium centers in both BS and triplet states (see Supporting Information). Our exchange constant calculations show that the magnetic properties of Torardi et al.[20] and Tennant et al.[22,23] structures can be well-described by an isolated dimer model.

This proposed magnetic model and the exchange constant values for the $D_O$ dimers are very different from our previous results[4] obtained from the Guliants et al.[24] structural data. A rather important value (77 K) for the exchange coupling constant of the $D_O$ dimer had been found, suggesting an alternating dimer chain along the *b* direction. Thus, the choice of the crystal data appears as a crucial issue for the determination of the adequate HDVV model. Comparing different structural data (Table 2), the main, still slight, variation within the $D_O$ dimers is found in the V−O−V angles. Being approximately 97° in the crystallographic data of Torardi et al.[20] and Tennant et al.,[22,23] it is equal to 94° in the data of Guliants et al.[24] It is known that even such a small M−L−M angle change in metal dimers can lead to drastic changes in the exchange parameter value, sometimes inverting the sign of the magnetic interaction.[35] The critical dependence of the exchange parameter on the V−O−V angle was demonstrated in our previous paper.[3] One should note that a relative variation of ≈20% in the intrachain $D_{OPO}$ exchange constant is observed between 10 K and room temperature. Such an observation stresses the limitation of any description of magnetic data neglecting the temperature dependence of exchange parameters.

**Fits of Temperature-Dependent $^{31}$P NMR Data.** As mentioned in a previous section, the NMR paramagnetic shift depends on two different ingredients, the hyperfine and exchange constants. Correspondingly, three levels of paramagnetic shift vs temperature data analysis can be suggested. First, all the parameters can be taken from ab initio calculations. Second, one can use the independently evaluated (theoretically or experimentally) magnetic exchange constants and then perform a numerical fit of the hyperfine parameters. The third possibility consists of the fitting of all the ingredients, namely, the hyperfine and exchange constant parameters. We previously used the first two strategies for the ambient pressure phases of $(VO)_2P_2O_7$,[2,5] $VO(HPO_4)\cdot 0.5H_2O$,[5] and $VO(H_2PO_4)_2$ [36] compounds.

In this paper, the third strategy is applied with a full fitting of all the parameters from the NMR data. Obviously, the knowledge of a sufficient number of experimental points in a wide range of temperature is a prerequisite. In the meantime, our ab initio calculations of exchange constants allow us to determine the underlying magnetic models with a minimal number of exchange parameters which are assumed to be temperature-independent. For the three magnetic models proposed before, the values of the fitted parameters are reported in Table 5 and the fitted curves ($\delta = f(T)$) together with the experimental data are given in Figure 4. From Table 5, one can see that the fit quality ($\mathscr{R}$) is comparable for the three proposed magnetic models. In addition, the hyperfine coupling constants and the temperature-independent shifts are very similar. On the basis of the coupled dimer chain models, the fitting leads to two

(35) Kahn, O. *Molecular Magnetism*; Wiley-VCH: New York-Chichester-Weinheim-Brisbane-Singapore-Toronto, 1993.
(36) Petit, S. Ph.D. Thesis, Ecole normale supérieure de Lyon, 2003.

**Table 5.** Extracted Parameter Values for the Three Proposed Magnetic Models[a]

| model | $A$ (MHz) | $\delta_{dia}$ (ppm) | $J$ (K) | $R$ |
|---|---|---|---|---|
| isolated dimer | $30.8 \pm 4$ | $-275 \pm 31$ | $88 \pm 1$ | $9.6 \times 10^{-5}$ |
| alternating dimer chain | $29.4 \pm 3$ | $-283 \pm 30$ | $89 \pm 1$ ($J_1$), $-38 \pm 3$ ($J_2$) | $5.0 \times 10^{-5}$ |
| coupled dimer chains | $28.8 \pm 4$ | $-289 \pm 30$ | $91 \pm 1$ ($J_1$), $-39 \pm 3$ ($J_2$), $-11 \pm 1$ ($J_3$) | $5.0 \times 10^{-5}$ |

[a] The error bars leading to a 10% variation of the $\mathcal{R}$ value are indicated.

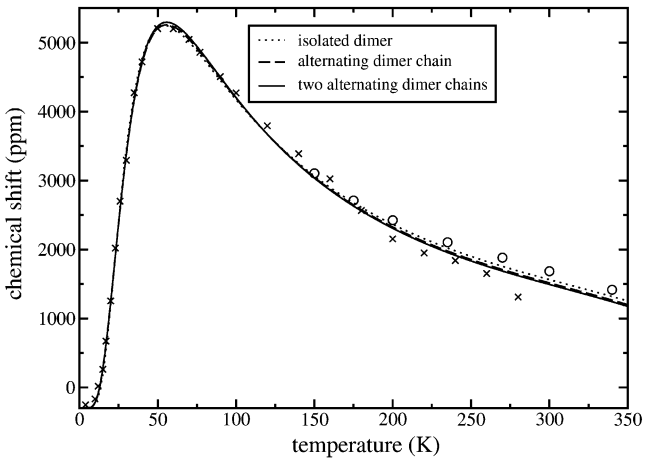


**Figure 4.** Fitting of the $^{31}P$ NMR data of Kikuchi et al.[27] The ○ and the × show the experimental values of refs 28 and 27, respectively.

intrachain parameters of comparable absolute values but of different nature (antiferromagnetic and ferromagnetic). Let us remind that these models were suggested by our calculations using Guliants et al.[24] structural data (see Table 4). However, both ab initio intrachain exchange constants are of antiferromagnetic nature. Thus, we believe that the coupled dimer chain picture should be ruled out. One can conclude that either the structure reported in ref 24 needs further investigations or several very similar structures are present. Finally, the isolated dimer model seems more adequate for the description of the magnetic properties of $VO(HPO_4)\cdot 0.5H_2O$. The exchange constant value of 88 K (attributed to the intrachain $D^1_{OPO}$ dimer) is very close to the values extracted from the magnetic susceptibility[13,15,25] and INS[22] measurements (see Table 1).

Our theoretical calculations combined with the fitting of the temperature-dependent NMR data allow to give a coherent description of the magnetic interaction scheme in $VO(HPO_4)\cdot 0.5H_2O$.

## 4. Conclusion

Using the different crystallographic structures of the vanadyl hydogenophosphate hemihydrate $VO(HPO_4)\cdot 0.5H_2O$ reported in the literature, we have performed DFT calculations of exchange coupling constants on three different types of extracted model dimers. The first important result is that the dominant exchange pathway occurs through intrachain double O−P−O bridges as in $(VO)_2P_2O_7$ solids. This conclusion differs from the previous extended Hückel based calculations which favored a different dominating exchange pathway. Our calculations emphasized that small geometrical variations lead to significant changes in the strength of the exchange coupling constants and thus to radically different magnetic schemes. These ab initio evaluations are extremely valuable in the determination of possible interaction patterns. Thus, assuming different magnetic schemes suggested by our ab initio investigations, we performed a complete fit of the experimental temperature-dependent NMR data to extract exchange as well as hyperfine constants. The comparison between the extracted exchange constant set and the ab initio ones suggested that NMR data were recorded on the crystallographic structures reported by Torardi et al.[20] and Tennant et al.[22,23] Finally, this work can be considered as (i) a validation of the combined DFT/BS numerical approach since good agreement between the calculated exchange constants and the extracted ones was reached; and (ii) an original strategy combining experimental NMR fit and ab initio calculations to clarify the magnetic properties of solids in relation with their crystallographic structures.

**Acknowledgment.** We wish to thank S. E. Nagler for making available the crystal structures of $VO(DPO_4)\cdot 0.5D_2O$. We are also grateful to J. Kikuchi for providing us the NMR data for $VO(HPO_4)\cdot 0.5H_2O$.

**Supporting Information Available:** Spin densities on the vanadium atoms and their first coordination spheres. This material is available free of charge via the Internet at http://pubs.acs.org.

IC035437X